World Academy of Science, Engineering and Technology
International Journal of Energy and Environmental Engineering
Vol:12, No:4, 2018

# Study on the Integration Schemes and Performance Comparisons of Different Integrated Solar Combined Cycle-Direct Steam Generation Systems

Liqiang Duan, Ma Jingkai, Lv Zhipeng, Haifan Cai



***Abstract*—**The integrated solar combined cycle (ISCC) system has a series of advantages such as increasing the system power generation, reducing the cost of solar power generation, less pollutant and $CO_2$ emission. In this paper, the parabolic trough collectors with direct steam generation (DSG) technology are considered to replace the heat load of heating surfaces in heat regenerator steam generation (HRSG) of a conventional natural gas combined cycle (NGCC) system containing a PG9351FA gas turbine and a triple pressure HRSG with reheat. The detailed model of the NGCC system is built in ASPEN PLUS software and the parabolic trough collectors with DSG technology is modeled in EBSILON software. ISCC-DSG systems with the replacement of single, two, three and four heating surfaces are studied in this paper. Results show that: (1) the ISCC-DSG systems with the replacement heat load of HPB, HPB+LPE, HPE2+HPB+HPS, HPE1+HPE2+ HPB+HPS are the best integration schemes when single, two, three and four stages of heating surfaces are partly replaced by the parabolic trough solar energy collectors with DSG technology. (2) Both the changes of feed water flow and the heat load of the heating surfaces in ISCC-DSG systems with the replacement of multi-stage heating surfaces are smaller than those in ISCC-DSG systems with the replacement of single heating surface. (3) ISCC-DSG systems with the replacement of HPB+LPE heating surfaces can increase the solar power output significantly. (4) The ISCC-DSG systems with the replacement of HPB heating surfaces has the highest solar-thermal-to-electricity efficiency (47.45%) and the solar radiation energy-to-electricity efficiency (30.37%), as well as the highest exergy efficiency of solar field (33.61%).

***Keywords*—**HRSG, integration scheme, parabolic trough collectors with DSG technology, solar power generation.

## I. Introduction

IN recent years, the integration of solar energy into fossil fueled plants are paid an increasing attention by researchers aiming to find a better way of using solar energy. Integrated solar combined cycle systems (ISCCS) can not only achieve higher conversion efficiencies of solar radiation energy into electricity, but also eliminate the thermal storage system and reduce the cost of solar thermal power generation. Baghernejad and Yaghoubi studied the ISCC system in Yazd, Iran, and found that low exergy efficiency subsystems which included the combustion chambers, mirrors and heat exchangers [1]. Giovanni Manente studied a 390 MWe natural gas combined cycle (NGCC) with a three-pressure heat recovery steam generator (HRSG), finding that the maximum power generation capacity of solar energy was 19 MWe without changing the system; at the same time, different concentrating solar power (CSP) technologies were considered to replace the heat load of different heating surfaces of the HRSG, and they concluded that it was possible to reduce the irreversible loss of the HRSG by adopting a solar collector technology with the suitable temperature [2], [3]. Mario Amelio proposed a new system in which the compressed air is heated by linear Fresnel-type collectors before entering into the combustion chamber, which has a certain advantage over replacing heating surfaces of the HRSG [4]. Lin Rumou outlined the solar energy and combined cycle thermal complementary concept from the system level in accordance with the solar concentrating process and energy complementary model [5]. Allani et al. has studied both the efficiency and economic feasibility of implanting the heat transfer fluid-ISCCS (HTF-ISCCS) and found the maximum power strategy offers higher potential for $CO_2$ mitigation than the maximum efficiency and the more economic plant corresponds to smaller solar field [6]. Kane and Favrat proposed the use of higher pressure steam cycle to improve the exergy efficiency because they found that the exergy losses in the heat exchangers network strongly depends on the solar thermal energy input from the solar field [7]. Khaldi has carried out the energy and exergy analysis of the first HTF-ISCCS in Algeria and revealed that the combustor of the gas turbine and the solar field are the major sources of the energy and exergy losses [8]. Bakos and Parsa have revealed that the fuel saving mode can provide the lower LEC than the power boosting mode and the larger solar field leads to the higher the cost of electricity production from the economic analysis of HTF-ISCCS and the effect of solar field size on the costs of the power plant in Southern Greece [9]. Antoñanzas-Torres et al. have investigated the impact of direct solar radiation (DNI), the solar field size and ambient temperature on the performance of the HTF-ISCCS operating in power boosting mode, finding the CC power plant in Las Vegas has the lower performance than the one in Ciudad Real due to the higher temperatures, whereas the ISCCS offers better performance in Las Vegas than in Ciudad Real because of the higher DNI [10]. Reddy found that both the energetic and exergetic efficiencies of the HTF-ISCCS are lower compared to those of conventional combined cycle [11]. Cau Giorgio et al. revealed that the use of solar energy for producing steam offers better performance than the case of

Liqiang Duan is with the School of Energy Power and Mechanical Engineering, North China Electric power University, Beijing, 102206,P.R.China (corresponding author, phone: 8610-61771443; fax: 8610-61772383; e-mail: dlq@ncepu.edu.cn).

Jingkai Ma, Zhipeng Lv, and Haifan Cai are with the School of Energy Power and Mechanical Engineering, North China Electric Power University, Beijing, 102206, P. R. China (e-mail: majingkai886@163.com, 18501315443@163.com, 13718870221@163.com).

preheating, evaporating and superheating water/steam using $CO_2$ as a heat transfer fluid [12]. Feldhoff Jan Fabian pointed out the DSG (direct steam generator) technology is more promising than the HTF technology, since it does not require the heat exchangers and can lead to an increase in the operation temperature of the Rankine cycle (above 400°C) [13]. El-Sayed concluded that the performance of DSG-ISCCS with the power boosting mode was more economical than that in the fuel saving mode and DSG-ISCCS can become economically feasible if the cost of solar field is decreased and the natural gas prices increases [14]. Livshits concluded that the overall energy conversion efficiency of 40–55% is feasible and the solar fraction up to 50% can be reached at a new concept system that uses the solar radiation collector by the medium-temperature parabolic trough solar field to enhance the thermodynamic performance of steam-injection gas turbine [15]. Li Yuanyuan proposed a novel ISCCS where the two-stage DSG technology is integrated into the double-pressure HRSG, and the low pressure and reheat pressure are optimized to obtain the optimized operating parameters of the ISCC system [16]. Nezammahalleh et al. found that the DSG-ISCCS has better performance than HTF-ISCCS [17]. Kelly et al. concluded the most efficient use of solar thermal energy is to product the high pressure saturated steam for the heat recovery steam generator and small annual solar thermal contributions to an integrated plant can be converted to the electric energy at a higher efficiency than a solar-only parabolic trough plant [18].

Both the efficiency and economic performance researches of ISCCS with the replacement of single heating surface using parabolic trough collectors are paid too much attention. However, the research on ISCCS with the replacement of multi-stages heating surfaces is almost ignored. It is unknown that whether the use of solar energy alternative heating surfaces will have a certain advantage. Thus, this paper mainly studies the ISCC-DSG systems with the heat load replacement of single, two, three and four heating surfaces and compares their performances.

## II. System Description

### *A. The Reference Natural Gas Combined Cycle*

The reference NGCC plant consists of a General Electric PG9351 gas turbine, a triple-pressure HRSG with reheat. Fig. 1 shows the flowsheet of the reference NGCC plant. the feed water enters into the low pressure economizer (LPE) after being pressured by the low pressure feed water pump, and is divided into three parts at the outlet of LPE: the low pressure feed water, the intermediate pressure feed water and the high pressure feed water. The low pressure feed water enters into the low pressure evaporator (LPB) for evaporation and finally becomes the superheated steam in the low pressure superheater (LPS). The superheated steam is mixed with the exhaust steam leaving the intermediate pressure turbine (IPT) and sent to the low pressure turbine (LPT). The intermediate pressure feed water enters into the intermediate pressure feed water pump, followed by the intermediate pressure economizer (IPE), the intermediate pressure evaporator (IPB) and the intermediate pressure superheater (IPS), finally it turns into the in intermediate pressure superheated steam. The intermediate pressure superheated steam is mixed with the exhaust steam leaving the high pressure turbine (HPT) and reheated in reheater1 (RH1) and reheater2 (RH2) before entering into the intermediate pressure turbine (IPT); the high pressure feed water enters into the high-pressure feed pump, followed by the high pressure economizer1 (HPE1), high pressure economizer2 (HPE2), high pressure evaporator (HPB), high pressure superheater1 (SH1) and high pressure superheater2 (SH2), finally it is changed into the high pressure superheated steam and sent to the HPT.

The reference NGCC plant mode is established by Aspen Plus software. The model of HRSG is shown in Fig. 2. The design parameters (as shown in Table I) are based on the actual power plant operation data. The system power output is 253.9 MW and the exhaust gas temperature of gas turbine is 609.4°C.

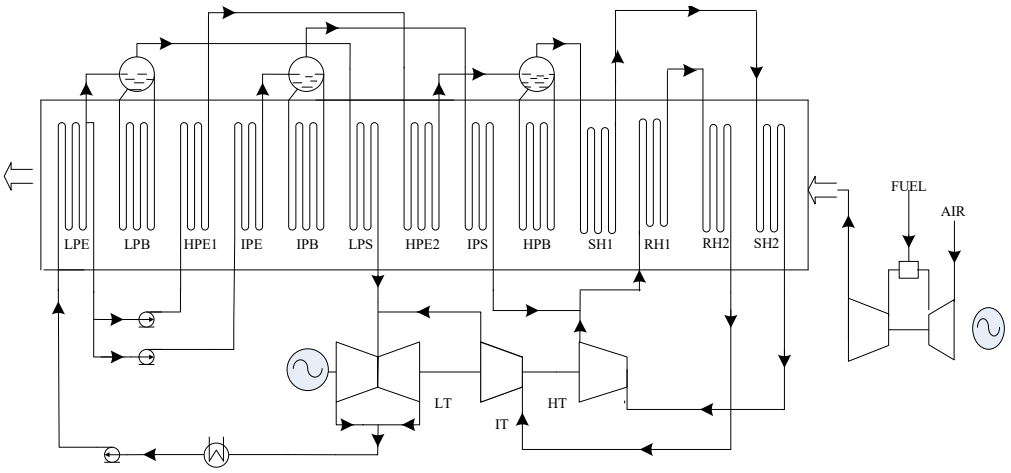


Fig. 1 Flowsheet of the reference NGCC plant

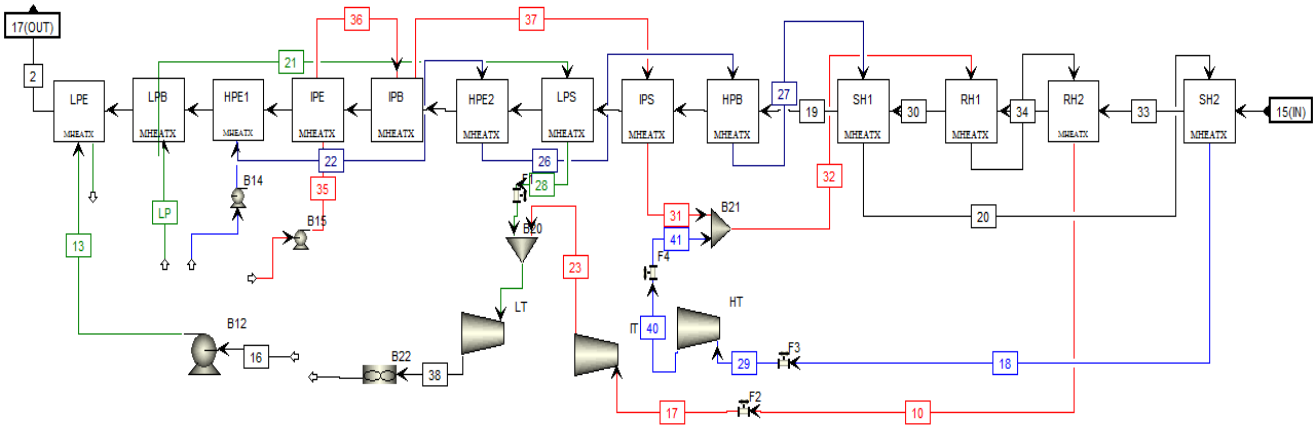


Fig. 2 Model of HRSG built in Aspen Plus software

TABLE I
GAS TURBINE AND STEAM BOTTOMING CYCLE SYSTEM DESIGN PARAMETERS

| | PARAMETERS | Value |
|---|---|---|
| Gas turbine | Pressure ratio | 15.4 |
| | Turbine inlet temperature (°C) | 1318 |
| | Turbine exhaust temperature (°C) | 609 |
| | Air flow (kg/s) | 623.7 |
| | Exhaust gas mass flow (kg/s) | 637.78 |
| | Generator power output (MW) | 255.6 |
| | System efficiency (%) | 36.09 |
| Steam cycle system | Steam pressure (High / Intermediate / Low, MPa | 9.99/2.4/0.4 |
| | Superheated steam temperature (High / Intermediate / Low, °C) | 540.8/301.6/300 |
| | Reheat steam temperature (°C) | 542.8 |
| | Pinch point temperature difference (°C) | 12 |
| | Approach point temperature difference (°C) | 8 |
| | Isentropic efficiency of steam turbine（High / Intermediate / Low) | 0.875/0.895/0.89 |

Fig. 3 shows the temperature-heat load (T-q) diagram in the HRSG of the NGCC. Both the pressure loss and heat loss between the flue gas and water/steam are neglected in the heating surface of HRSG. The exhaust gas temperature of HRSG is 87.56°C. The majority of the heat that flue gas releases is used for evaporation and superheating of the high pressure feed water and reheat of reheat steam. The feed water mass flow rates of low pressure, intermediate pressure and high pressure are 10.71 kg/s, 11 kg/s and 78.95 kg/s, respectively. The power output of the steam turbine is 134.742 MW.

### *B. The Solar Energy Field*

The solar energy field is composed of the parabolic trough collectors with the DSG technology that includes the typical ET-150 solar collectors. Their geometrical and optical parameters are shown in Table II. The ET-150 solar collectors have been applied in the DSG solar collector field of German Aerospace Center (DLR) and are validated in detail at the solar steam (DISS) test facility. The geometric concentration ratio defined as the ratio of collector aperture width (5.77 m) the receiver outside diameter (0.07 m) is 82. The peak optical efficiency is 75%. A fraction of feed water or steam leaving heating surfaces of HRSG is heated to the specified in the receivers of the solar energy field and then returned to other heating surface of the HRSG. The solar energy field a role of replacing part of the heating load of the HRSG. The parabolic trough collectors with the DSG technology are modeled in EBSILON software, as shown in Fig. 4.

TABLE II
THE GEOMETRICAL AND OPTICAL PARAMETERS OF ET-150 SOLAR COLLECTORS

| PARAMETERS | Value |
|---|---|
| Absorber tube outer diameter (m) | 0.07 |
| Absorber tube inner diameter (m) | 0.055 |
| Glass envelope outer diameter (m) | 0.115 |
| Glass envelope inner diameter (m) | 0.109 |
| Reflector aperture width (m) | 5.77 |
| Length of each module (m) | 12.27 |
| Length of mirror in each module | 11.9 |
| Mirror reflectivity | 0.92 |
| Glass transmissivity | 0.945 |
| Solar absorptivity | 0.94 |
| Peak optical efficiency | 0.75 |
| Absorber tube outer diameter (m) | 0.07 |
| Absorber tube inner diameter (m) | 0.055 |

TABLE III
THE KEY PARAMETERS FOR THE DESIGN POINT

| Design point parameters | Yinchuan (China) |
|---|---|
| Direct normal irradiation (W/m$^2$) | 850 |
| Latitude (°C) | 38.47 |
| Longitude (°C) | 106.27 |
| Ambient temperature (°C) | 25 |
| Sun height angle (°C) | 70.28 |
| Sun azimuth angle (°C) | 224.72 |
| Incidence angle (°C) | 13.87 |

The location chosen for this study is Yinchuan, the provincial capital of Ningxia province in China. The weather data at noon on June 21$^{st}$, when the DNI is 850 W/m$^2$ is selected as the solar energy field design point. The key parameters for the design point are shown in Table III.

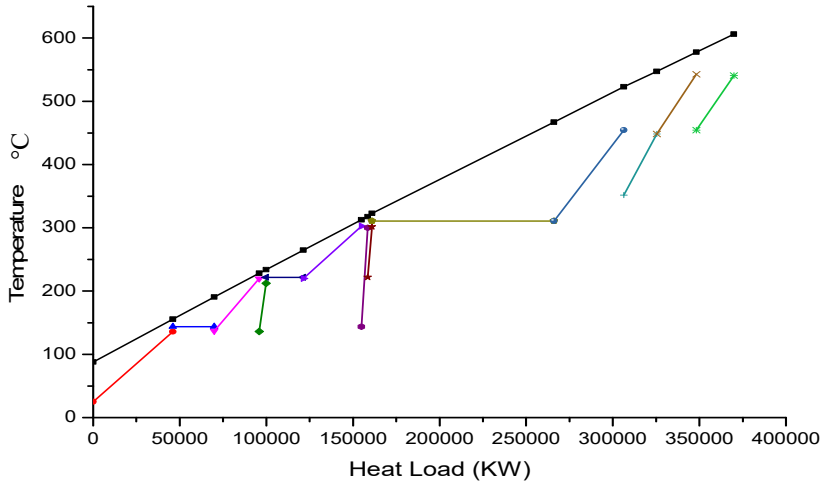


Fig. 3 Temperature-heat load (T-q) diagram in the HRSG of the NGCC

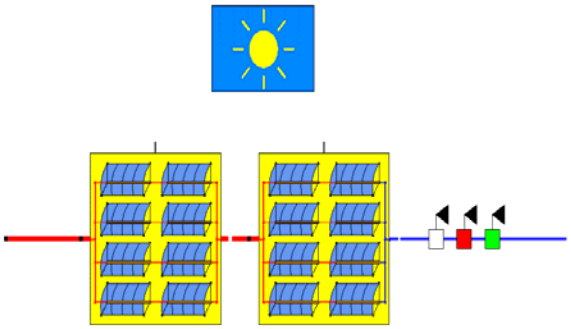

Fig. 4 Model of Parabolic trough collectors with DSG technology

## III. Performance Evaluation Criteria

Both the energy and exergy analysis methods are used to assess the performance of the ISCCS.

### *A. Energy Analysis*

The energy conversion efficiency of the solar radiation energy into electricity ($\eta_{sol-e}$) is defined as the ratio of the electricity that is the increased power output of the steam bottoming cycle in the ISCC plant compared to the reference NGCC plant to the solar radiation energy:

$$\eta_{sol-e} = \frac{\Delta E}{R_{solar}} = \frac{\Delta E}{A_{coll} * DNI_{inc}} \quad (1)$$

where, $\Delta E$ is the increased power output of the steam bottoming cycle in the ISCC plant compared to the reference NGCC plant. $R_{solar}$ is the inputted the solar radiation energy. $A_{coll}$ is the area of the solar collectors.

The energy conversion efficiency of the solar thermal energy into electricity ($\eta_{th-e}$) is defined as the ratio of the electricity that is the increased power output of the steam bottoming in the ISCC plant compared to the NGCC plant to the solar thermal energy:

$$\eta_{th-e} = \frac{\Delta E}{Q_{sol,th}} \quad (2)$$

The solar energy field efficiency ($\eta_{field}$) is defined as the ratio of the solar thermal energy to the solar radiation energy:

$$\eta_{field} = \frac{Q_{sol,th}}{A_{coll} * DNI_{inc}} \quad (3)$$

The proportion of the electricity that generated by the solar energy in the total power output is defined as the share of solar power ($\chi_{el-th}$), $E_{iscc}$ is the total power output of the ISCC plant.

$$\chi_{el-th} = \frac{\Delta E}{E_{iscc}} \quad (4)$$

### *B. Exergy Analysis*

The exergy efficiency is defined as the ratio of $\Delta E_{xe}$ (earnings) to $\Delta E_{xp}$ (pay), where:

$$\Delta E = (h1 - h2) - T0(S1 - S2) \quad (5)$$

For the heating surface of HRSG, the exergy efficiency is defined as the ratio of $E_{xws}$ to $E_{xflue}$,where, $E_{xws}$ is the exergy water/steam obtained from the heating surface of HRSG and $E_{xflue}$ is the exergy available from the exhaust gas in the heating surface of HRSG:

$$\eta_{ex-HRSG} = \frac{E_{xws}}{E_{xflue}} \quad (6)$$

where, $E_{ex-sol}$ is the exergy of solar energy field and $\eta_{ex-sol}$ is defined as the ratio of $E_{sol}$ to $E_{xsol-inc}$,where, is the increased exergy of water/steam in the DSG parabolic trough collectors and $E_{xsol-inc}$ is the exergy of the solar irradiation energy,

$$\eta_{ex-sol} = \frac{E_{sol}}{E_{xsol-inc}} \quad (7)$$

$$E_{xsol-inc} = A_{coll} * DNI_{inc} * \left[1 - \frac{4}{3}\frac{T_0}{T_S} + \frac{1}{3}\left(\frac{T_0}{T_S}\right)^4\right. \quad (8)$$

where, $T_S$ is the sun surface temperature (about 5276 K) and $T_0$ is the reference ambient temperature (298 K).

## IV. Research on Different Integration Schemes

### A. Replacing One Heating Surface of HRSG

1) Heat Load Distribution of the Reference NGCC System

There is a big difference in the heat load distribution between the different heating surfaces of the HRSG of the reference NGCC. The proportions of the absorbed heat of different heating surfaces in the total released heat of the flue gas in HRSG are shown in Fig. 5. According to the Fig. 5, the heat transfer quantities in the heating surfaces of SH2, RH2, RH1, SH1, HPB, HPE2, IPB, HPE1, LPB and LPE, are much greater than those in the heating surfaces of LPE, LPS and IPS. The heat transfer quantity of HPB is the largest accounting for 28.37% of the total released heat of the flue gas. Because the proportions of the absorbed heat of LPE, LPS, IPS heating surfaces in the total released heat of the flue gas are 1.06%, 0.98%, and 0.67%, respectively, using the solar energy field to replace the heat load of LPE, LPS, IPS heating surfaces has almost no effect on the reference NGCC, it is not suitable to use the solar energy field to replace the heat load of LPE, LPS, IPS, respectively. Both the first stage steam superheater (SH1) and the first stage steam reheater (RH1) are considered feasible to be heated by the parabolic trough collectors with DSG technology. The steam temperature is not able to reach the temperature of steam leaving SH2 (540.8°C) and RH2 (542.8°C), thus replacing the SH2 and RH2 is not considered.

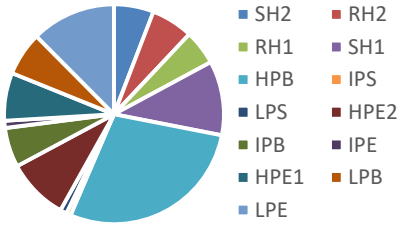


Fig. 5 Proportions of the absorbed heat of different heating surfaces in the total released heat of the flue gas in HRSG

2) Integration Scheme of Replacing one Heating Surface of HRSG

The parabolic trough collectors with DSG technology is used to replace part of heat loads of SH2, RH2, RH1, SH1, HPB, HPE2, IPB, HPE1, LPB and LPE heating surfaces respectively in order to find out the best ISCC layout. The coupling of DSG trough solar energy field with the bottoming steam cycle has some impacts on the reference NGCC system, which may result in the unsafe operation of the HRSG. Therefore, some control strategies are necessary for ISCC-DSG plants:

1) Both the pressure and temperature of the high/intermediate/low-pressure steam are constant.
2) Both the pinch point temperature difference and the approach point temperature difference are unchanged.
3) The heat transfer temperature difference at the end of each heating surface is greater than 8°C.
4) In consideration of the low temperature corrosion of the flue gas, the temperature of exhaust gas is greater than 80°C.

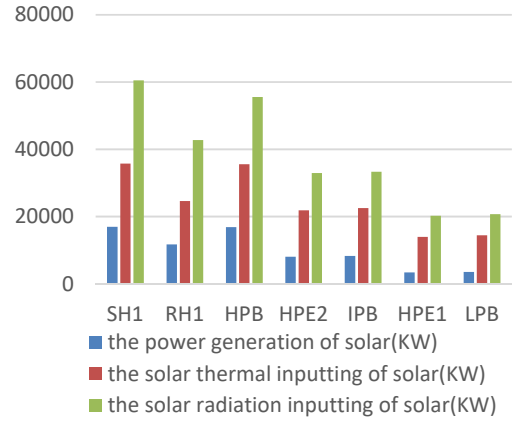


Fig. 6 Solar energy in ISCC-DSG systems with the replacement of one heating surface

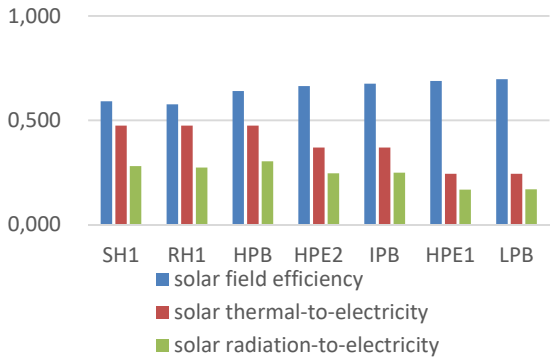


Fig. 7 Solar efficiency in ISCC-DSG systems with the replacement of one heating surface

Both Figs. 6 and 7 show the results of the stimulated ISCC-DSG systems with the replacement of single heating surface in HRSG. As shown in Fig. 6, the power generation of solar energy changes from 3.51 MW to 16.87 MW. When replacing SH1, RH1 and HPB alone, the limit of the exhaust gas temperature leads to the partial replacement of SH1, RH1 and HPB heating surfaces. The biggest power generation of solar energy (16.87 MW) and the highest thermo-electric conversion efficiency (30.4%) of solar energy are achieved in the ISCC-DSG system with the replacement of HPB heating surface. In order to ensure that the heat transfer temperature difference at the end of each heating surface, the parabolic trough collectors partially replace the heat loads of HPE2, IPB, HPE1 and LPB heating surfaces. As the energy level of solar thermal energy decreases, the conversion efficiency of solar thermal energy into the electricity decreases, whereas the lowest conversion efficiency of solar thermal energy into the electricity (24.3%) and the least power generation of solar (3.51 MW) are obtained by the ISCC-DSG system with the replacement of LPB heating surface.

When the parabolic trough collectors replace the heat loads

of different heating surfaces of HRSG, the temperature difference of the water/steam temperature in the tube of parabolic trough collectors leads to the different heat losses and the different solar energy field efficiencies in each different integration scheme. Fig. 7 shows the lowest solar energy field efficiency (57.7%) is obtained in the ISCC-DSG system with the replacement of RH1 heating surface due to the highest steam temperature in the tubes of the parabolic trough collectors, on the contrary, 69.7% is the highest solar energy field efficiency achieved in the ISCC-DSG system with the replacement of LPB heating surface due to the least heat loss in the tubes of parabolic trough collectors. The solar radiation energy-to-electricity efficiency calculated by combining the solar energy field efficiency and solar thermal energy-to-electricity efficiency varies between 16.75% achieved in ISCC-DSG system with the replacement of HPE1 heating surface and 30.37% achieved in ISCC-DSG system with the replacement of HPB heating surface. It clearly appears that ISCC-DSG system with the replacement of HPB heating surface is the best scheme under the replacement of one heating surface.

### *B. Replacing Two Heating Surfaces of HRSG*

As analyzed above, the ISCC-DSG system with the replacement of HPB heating surface has the highest solar radiation energy-to-electricity efficiency. Under the condition of replacing two heating surfaces of HRSG by using the parabolic trough collectors with DSG technology, in order to get the high solar thermal energy-to-electricity efficiency and solar radiation energy-to-electricity efficiency, one heating surface of HRSG is set to be HPB and the other heating surface is chosen from the remaining heating surfaces of HRSG, then ISCC-DSG systems with the replacements of HPB+SH1, HPB+RH1, HPB+HPE2, HPB+HPE1, HPB+IPB, HPB+ LPB and HPB+LPE heating surfaces are investigated. Among these integration schemes, the water/steam can flow through the HPB + HPS and HPB + HPE2 continuously, however, the water/steam cannot flow through HPB+RH1, HPB+HPE1, HPB+IPB, HPB+LPB, HPB+LPE continuously, where the different extraction ratios of water results in the different results. Some assumptions are made in this study as follows: the total solar radiation energy inputted to the RH, HPE1, IPB, LPB and LPE is consistent with the amount of solar radiation energy inputted to the HPE2 in order to compare the performance of each ISCC integration layout. Both the pinch point temperature difference and the approach point temperature difference are kept unchanged and the temperature of exhaust gas is greater than 80°C.

Both Figs. 8 and 9 show the power generation of solar energy and the efficiency of ISCC-DSG systems. The solar radiation energy inputted to the HPE2 is 12337.5 kW, and then the solar radiation energy inputted to RH, HPE1, IPB, LPB, and LPE is set to be 12337.5 kW. The total solar radiation energy inputted is composed of the solar radiation energy input for replacing the heat load of HPB and the solar radiation energy for replacing the heat load of other heating surfaces. The power generation of solar energy is limited by the exhaust gas temperance. The highest solar radiation energy-to-electricity efficiency (29.72%) is achieved in ISCC-DSG system with the replacement of HPB+RH1, which is still lower than that in ISCC-DSG system with the replacement of only HPB heating surface. The replacement of HPB+HPE1 heating surfaces obtains the lowest solar radiation energy-to-electricity efficiency (26.92%). The solar radiation energy-to-electricity efficiency of ISCC-DSG system with the replacement of HPB+LPE is 28.21%.

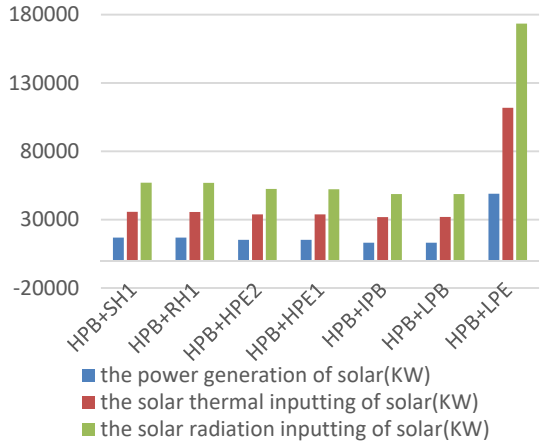


Fig. 8 The solar energy in ISCC-DSG systems with the replacement of two heating surfaces

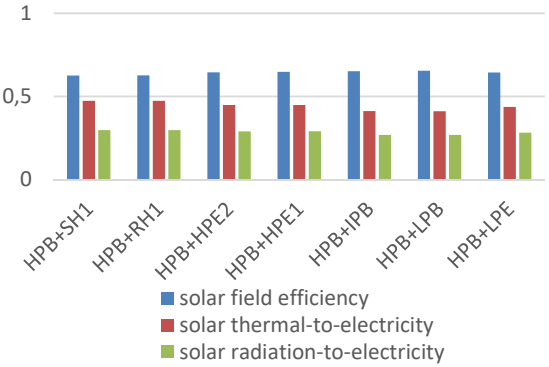


Fig. 9 Solar energy efficiency in ISCC-DSG systems with the replacement of two heating surfaces

The exhaust gas temperature of HRSG limits the further increase of solar power generation. For the integration scheme of HPB + LPE, the partial heat load replacement of LPE by the parabolic trough collectors reduces the influence of exhaust gas temperature on the ISCC system, resulting in extracting much more water leaving HPE2 into the solar energy field for evaporation. When the solar radiation energy input for replacing partial heat load of LPE heating surface is 12337.5 kW, the feed water with the mass flow rate of 21.88 kg/s is extracted from the feed water entering the LPE, at the same time, the mass flow of the feed water extracted from the HPE2 and evaporated in the solar energy field increases to 75.49 kg/s, leading a higher solar power generation of 48.99 MW that is much more than that in the ISCC-DSG system with the

replacement of HPB.

*C. Replacing Three Heating Surfaces of HRSG*

The parabolic trough collectors with DSG technology can also be used to replace the heat load of three heating surfaces of HRSG. If the replaced three heating surfaces of HRSG are not continuous, each heating surface with different mass flows of water/steam can be extracted, which will result in some controlling problems on the operation of HRSG, thus, three continuous heating surfaces of HRSG are selected for the performance analysis in this paper. Replacing the heating surfaces with the high temperature level has the higher solar radiation energy-to-electricity efficiency. So, the ISCC-DSG systems with the replacement of HPE1+HPE2+HP1, HPE2+HPB+SH1 and IPB+IPS+RH1 heating surfaces are selected and deeply investigated. Both the pitch point temperature difference and the approach temperature difference are kept unchanged and the temperature of exhaust gas is greater than 80°C.

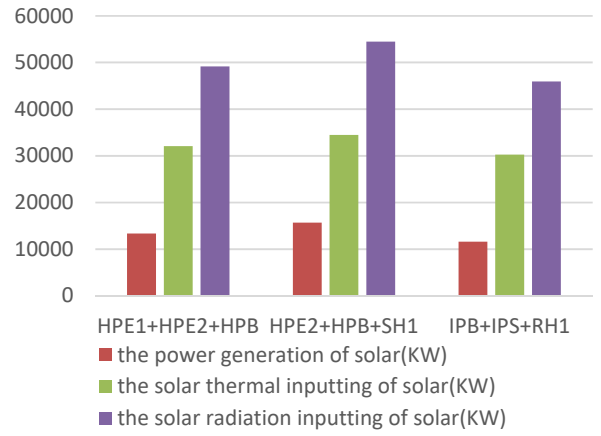


Fig. 10 Solar energy in ISCC-DSG systems with the replacement of three heating surfaces

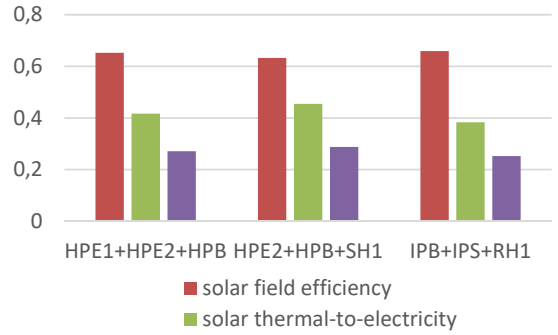


Fig. 11 Solar energy efficiency in ISCC-DSG systems with the replacement of three heating surfaces

Both Figs. 10 and 11 show the results for three kinds of ISCC system layouts with the replacement of three continuous heating surfaces of HRSG. The biggest power generation of solar energy (15.67 MW) and the highest solar radiation energy-to-electricity efficiency (28.76%) are achieved in the ISCC-DSG system with the replacement of HPE2+HPB+SH1. The high pressure feed water leaving HPE1 at 215°C is split into two streams: 1) one stream with the mass flow of 14.78 kg/s are preheated, evaporated and superheated up to 454.2°C in the solar energy field, the solar thermal energy adsorbed by the feed water is 34.46 MW; 2) the remaining steam with the mass flow of 74.84 kg/s goes through the same process in the HRSG. The least power generation of solar (11.61 MW) and the lowest solar radiation energy-to-electricity efficiency (25.57%) are obtained in the ISCC-DSG system with the replacement of IPB+IPS+RH1heating surfaces.

*D. Replacing Four Heating Surfaces of HRSG*

Four continuous heating surfaces of HRSG in are selected for the performance analysis. ISCC-DSG systems with the replacement of HPE1+HPE2+HPB+SH1, IPE+IPB+IPS+RH are chosen. Both the pitch point temperature difference and the approach temperature difference are kept unchanged and the temperature of exhaust gas is greater than 80°C.

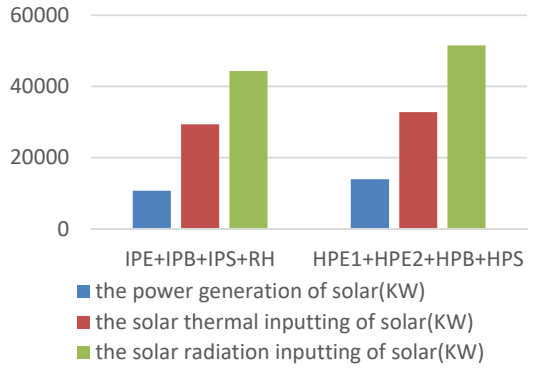


Fig. 12 Solar energy in ISCC-DSG systems with the replacement of four heating surfaces

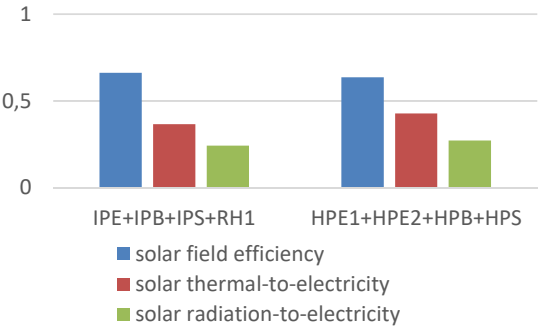


Fig. 13 Solar energy in ISCC-DSG systems with the replacement of four heating surfaces

Both Figs. 12 and 13 show the solar radiation energy-to-electricity efficiency of ISCC-DSG system with HPE1+HPE2+HPB+SH1 (27.2%) is 2.93% higher than that of ISCC-DSG system with IPE+IPB+IPS+RH1 (24.37%). In the ISCC-DSG system with the replacement of HPE1+HPE2+HPB+SH1, the feed water leaving the HP pump with the mass flow of 12.26 kg/s is preheated, evaporated and superheated to 454.4°C and mixed with the steam that undergoes the same process in the HRSG, which is further superheated to 540.2°C

in the HRSG. Both the solar radiation energy input and the solar thermal energy input are 51.52 MW and 32.75 MW, respectively, leading to the increased power generation of solar (about 14.01 MW).

## V. Performance Comparison of Optimal Integration Schemes for Replacing Different Heating Surfaces

It is necessary to compare the optimal integration scheme with different replacement modes of one, two, three, and four heating surfaces obtained from the above analysis to get the best integration scenarios under different requirements. ISCC-DSG system with the replacement of HPB, HPB+LPE, HPE2+HPB+SH1, HPE1+HPE2+HPB+SH1 heating surfaces shown in Table IV are analyzed and compared by using the energy and exergy analysis methods.

TABLE IV
ISCC-DSG Configurations

| Layout | Solar integration mode |
|---|---|
| ISCC1 | HPB |
| ISCC2 | HPB+LPE |
| ISCC3 | HPE2+HPB+SH1 |
| ISCC4 | HPE1+HPE2+HPB+SH1 |

### *A. Analysis of the Feed Water Flow and the Heat Load of HRSG*

Table V shows the mass flows of feed water under different integration schemes. The heat loads at the HRSG heating surfaces under different integration schemes are shown in Fig. 14, which shows that the inputting of solar energy has a certain effect on both the mass flow of feed water and the heat load on the HRSG heating surfaces. The biggest change of feed water flow and the heat load of the heat transfer surface is obtained in ISCC2.The mass flow of HP feed water increases from 78.95 kg/s to 120.79 kg/s, which results in a significant increase in the absorbed heat of HPE1, HPE2, SH1, SH2, RH1 and RH2 heating surfaces, resulting in a significant decrease in the absorbed heat in the remaining heating surfaces and the obvious decreases of the mass flows of both IP feed water and LP feed water. In the ISCC2 system, the HP feed water (120.79 kg/s) leaving HPE2 is split into two streams: 1) one part with the mass flow of 75.49 kg/s is evaporated in solar energy field, replacing part of heat load of HPB, 2) the other part with the mass flow of 45.3 kg/s is evaporated in the HRSG, causing that the heat load of HPB heating surface is significantly lower than that of the reference system.

TABLE V
Mass Flow of Feed Water of ISGG System

| Mass flow | NGCC | ISCC1 | ISCC2 | ISCC3 | ISCC4 |
|---|---|---|---|---|---|
| feed water (kg/s) | 10.71 | 8.88 | 5.39 | 8.86 | 11.14 |
| IP feed water (kg/s) | 11 | 8.29 | 3.14 | 12.15 | 11.63 |
| HP feed water (kg/s) | 78.95 | 93.37 | 120.79 | 89.61 | 87.86 |
| HP feed water heated by solar (kg/s) | / | 26 | 75.49 | 14.78 | 12.26 |

Both the changes of feed water flow and the heat load of the heat transfer surfaces in ISCC1 system are greater than those in ISCC3 and ISCC4. The mass flow rate of HP feed water increases from 78.95 kg/s to 93.37 kg/s. The inputting of solar energy has less influence on both the feed water flow rate and internal heat transfer of HRSG in both ISCC3 and ISCC4 systems. The least influence of the inputting of solar energy on the HRSG is achieved in ISCC4 system, indicating that both the changes of feed water flow and the heat load of the heat transfer surface in ISCC-DSG systems with the multi-stage heating surfaces replacement are smaller.

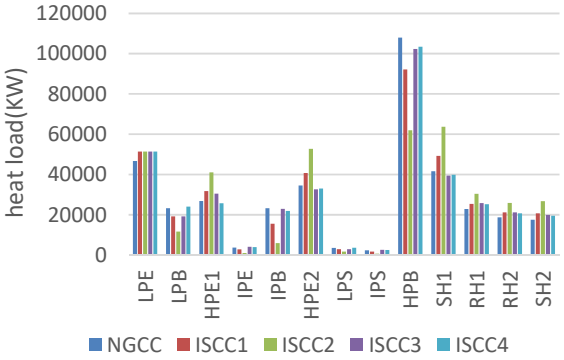


Fig. 14 Heat load of the heating surface of the HRSG under different integration schemes

### *B. Energy Analysis*

Table VI shows the results of the energy analysis for these five ISCC systems. The power output of steam bottoming cycle varies between 149.27 MW and 185.31 MW. The ISCC2 system has the greatest solar power output of 58.63 MW due to the use of the parabolic trough collectors with DSG technology to replace part of the heat load of the LPE; which results in more feed water leaving HPE2 is evaporated in solar energy field. Both the solar radiation energy and thermal energy input under this system are 205.72 MW and 132.62 MW, respectively. Limited by the temperature of exhaust gas, the solar power output in ISCC1 is 16.87 MW, which is greater than those in both ISCC3 (15.67 MW) and ISCC4 (14.01 MW) because the energy level of solar thermal energy used to heat water in both ISCC3 and ISCC4 is lower.

The solar energy field efficiency ($\eta_{field}$) changes from 63.24% to 64.47% depending on the temperature of water/steam in the tube of parabolic trough collectors. Because the heat loss in solar energy field replacing part of heat load of the LPE is less than that in solar energy field replacing part of heat load of the SH1, ISCC2 has the highest solar energy field efficiency (64.47%) and ISCC3 has the lowest solar energy field efficiency (63.24%). The solar-thermal energy-to-electricity efficiency ($\eta_{th\text{-}E}$) is in the range of 42.78% to 47.75%. The highest solar-thermal energy-to-electricity efficiency (47.45%) is gained in the solar energy field of ISCC1 due to the highest average heat absorption temperature, whereas the lowest average heat absorption temperature brings about the lowest solar-thermal energy-to-electricity efficiency (42.78%) obtained in the solar energy field of ISCC4.The maximum solar radiation energy-to-electricity efficiency (30.37%) is achieved in ISCC1, which is greater than that of the

independent solar energy plant and shows the advantage in the integration of solar energy with NGCC. The solar radiation energy-to-electricity efficiency of ISCC2 with the greatest power output is 28.22%.

### *C. Exergy Analysis*

Table VII shows the results of the exergy analysis for these five ISCC systems. The addition of solar energy to NGCC makes the exergy released by the flue gas in the HRSG increased to 182.93 MW, which is about 900 kW greater than that of the reference NGCC system. The results of the exergy analysis in HRSG of the reference NGCC system is shown in Fig. 15, the exergy efficiency of HRSG ($\eta_{Ex\text{-}HRSG}$) is 87.69%. The exergy efficiency of ISCC-DSG systems is higher than that of the reference NGCC system indicating that the addition of solar energy can play an important role in reducing the irreversible loss of HRSG. The introduction of solar energy has different impacts on the exergy transfer and distribution of flue gas in HRSG of different ISCC-DSG systems. ISCC2 has the highest exergy efficiency (90.72%) of HRSG, which has the greatest solar energy input leading to the greatest exergy of flue gas released in SH1/RH1/RH2/SH1 heating surfaces and the least exergy of flue gas released in HPB compared to other ISCC-DSG systems. Fig. 16 shows the exergy exchange results in each heating surface of ISCC2, the irreversible exergy loss of HRSG in ISCC2 is decreased to 16.97 MW from 22.47 MW. The exergy efficiency of HRSG ($\eta_{Ex\text{-}HRSG}$) of ISCC3 is 88.13%. The exergy exchange results in each heating surface of ISCC3 are shown in Fig. 17. The least exergy efficiency of HRSG (87.93%) is obtained in ISCC4 system due to the greatest exergy of flue gas is released in heating surface with the low exergy efficiency, as displayed in Fig. 18.

TABLE VI
PERFORMANCE COMPARISON OF ISCC-DSG SYSTEMS ON THE ENERGY ANALYSIS

| Parameters | NGCC | ISCC1 | ISCC2 | ISCC3 | ISCC4 |
|---|---|---|---|---|---|
| $E_{ST\text{-}gross}$ (kW) | 135813.62 | 157236.99 | 185312.26 | 151627.29 | 149943.72 |
| $E_{pump}$ (kW) | 1071.43 | 1252.66 | 1591.13 | 1213.41 | 1190.02 |
| $E_{ST\text{-}net}$ (kW) | 134742.19 | 155984.33 | 183721.13 | 150413.88 | 148753.70 |
| $E_{solar}$ (kW) | / | 16870.11 | 48978.94 | 15671.69 | 14011.51 |
| $S_{COLL}$ ($m^2$) | / | 65341.30 | 204220.94 | 64109.59 | 60608.82 |
| $R_{solar}$ ($kW_{th}$) | / | 55540.11 | 173587.80 | 54493.15 | 51517.50 |
| $Q_{sol.th}$ ($kW_{th}$) | / | 35556.78 | 111909.41 | 34462.76 | 32749.70 |
| $\eta_{field}$ (%) | / | 64.02 | 64.47 | 63.24 | 63.57 |
| $\eta_{ra\text{-}E}$ (%) | / | 47.45 | 43.77 | 45.47 | 42.78 |
| $\eta_{th\text{-}E}$ (%) | / | 30.37 | 28.22 | 28.76 | 27.20 |
| $\eta_{share}$ (%) | / | 10.82 | 26.66 | 10.42 | 9.42 |

TABLE VII
PERFORMANCE COMPARISON OF ISCC-DSG SYSTEMS ON THE EXERGY ANALYSIS

| Parameter | NGCC | ISCC1 | ISCC2 | ISCC3 | ISCC4 |
|---|---|---|---|---|---|
| $E_{Xfg}$ ($kW_{th}$) | 182174.5 | 182925.8 | 182932.2 | 182932.2 | 182932.2 |
| $E_{Xsteam\text{-}HRSG}$ | 159703 | 160919 | 165964 | 161222 | 160855 |
| $\eta_{Ex\text{-}HRSG}$ | 87.67 | 87.97 | 90.72 | 88.13 | 87.93 |
| $E_{Xsol.inc}$ ($kW_{th}$) | | 51777.88 | 161829.14 | 50801.84 | 48027.76 |
| $E_{Xsol}$ | | 17401.98 | 51824.74 | 16913.32 | 15423.58 |
| $\eta_{Ex\text{-}sol}$ | | 33.61 | 32.02 | 33.29 | 32.11 |
| $\eta_{sol+HRSG}$ | | 75.98 | 63.17 | 76.21 | 76.32 |

The exergy efficiency of solar energy field ($\eta_{Ex\text{-}sol}$) is significantly lower than that of HRSG due to that the majority of exergy of solar radiation cannot be transferred into the water/steam using the current CSP technology, which depends on both the optical and thermal characteristic of solar collectors and the temperature of water/steam heated in the tubes of solar field. The weather condition and the parabolic trough collectors selected in this study are all the same for ISCC-DSG, thus, the difference of exergy efficiency of solar energy field is caused from the different temperature of water/steam heated in the tubes of solar field. The highest exergy efficiency of solar field (33.61%) is achieved in ISCC1 for the highest temperature of water/steam heated in the tubes of solar field. The exergy efficiency of the solar field is decreased with the replacement of the low temperature heating surfaces, and the lowest exergy efficiency of solar field (32.02%) is obtained in ISCC2.

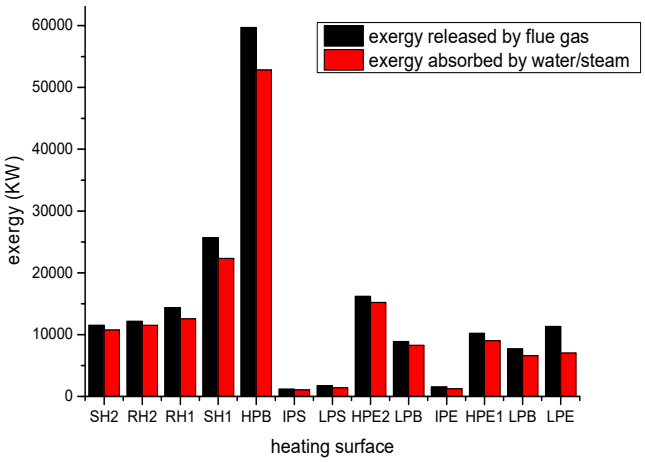


Fig. 15 Results of the exergy exchange in HRSG of the reference NGCC system

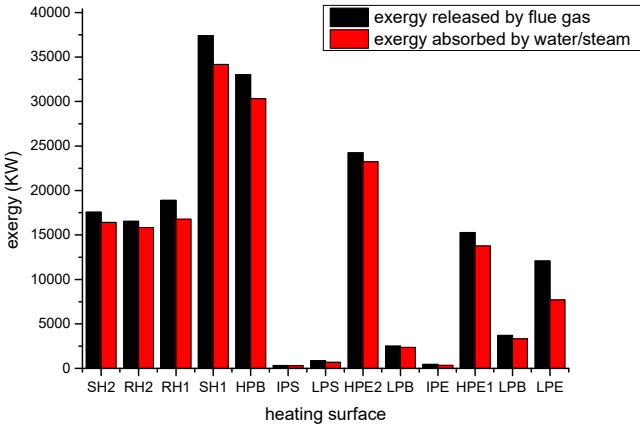


Fig. 16 Results of the exergy exchange in HRSG of the ISCC-DSG system with the replacement of HPB+LPE

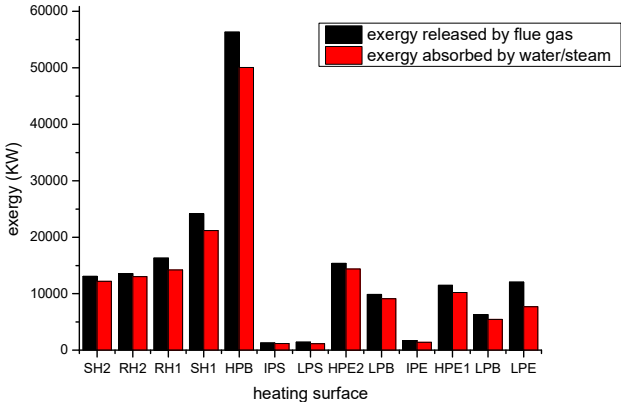


Fig. 17 Results of the exergy exchange in HRSG of the ISCC-DSG system with the replacement of HPE2+HPB+SH1

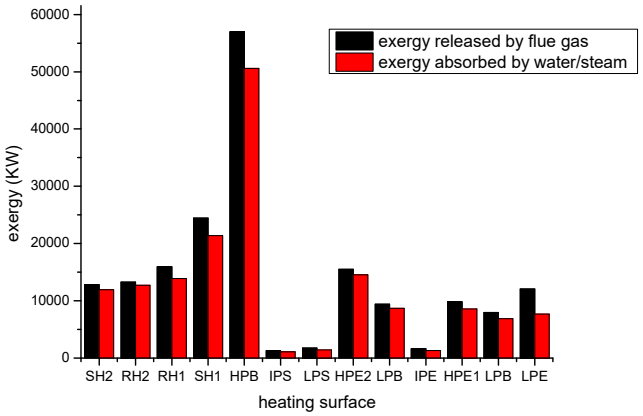


Fig. 18 Results of the exergy exchange in HRSG of the ISCC-DSG system with the replacement of HPE1+HPE2+HPB+SH1

## VI. Conclusion

This paper investigates the possible integration schemes of using the parabolic trough collectors with DSG technology to replace the heat load of heating surfaces in HRSG of a conventional NGCC system containing a PG9351FA gas turbine and a triple pressure reheat steam cycle. ISCC-DSG systems with the replacement one, two, three and four heating surfaces are studied in this paper, and the optimal schemes under different ISCC-DSG systems are obtained by the detailed energy and exergy analysis. The main conclusions are as follows:

1) The ISCC-DSG systems with the replacement of HPB, HPB+LPE, HPE2+HPB+HPS, HPE1+HPE2+ HPB+HPS are the best integration scenarios when the heat load of one, two, three and four stages of heating surfaces are partly replaced by the parabolic trough collectors with DSG technology, respectively.
2) Both the change of the feed water flow and the heat load of the heating surfaces in ISCC-DSG systems with the replacement of multi-stage heating surfaces have smaller change than those in ISCC-DSG systems with the replacement of a single heating surface.
3) The ISCC-DSG system with the replacement of HPB+LPE heating surfaces with the solar irradiation energy of 173.59 MW has the greatest solar power output of 58.63 MW because the use of parabolic trough collectors with DSG technology to replace part of the heat load of the LPE can reduce the constraint of the temperature of exhaust gas. The result shows that the ISCC-DSG system with the replacement of HPB+LPE heating surfaces can increase the solar power output significantly.
4) The ISCC-DSG system with the replacement heat load of HPB heating surface has the highest solar-thermal energy-to-electricity efficiency (47.45%), the highest solar radiation energy-to-electricity efficiency (30.37%), as well as the highest exergy efficiency of solar energy field (33.61%), indicating the advantage in the integration of solar energy with NGCC and the solar energy field is not suitable for being used to replace SH1, RH1 heating surfaces in HRSG.

## Acknowledgments

This study has been supported by the National Nature Science Foundation Projects (No. 51576062) and the National Key Research and Development Plan of China (No. 2017YFB0602101).

## References

[1] A Baghernejad, M Yaghoubi, Exergy analysis of an integrated solar combined cycle system (J). Renewable Energy, 2010; 35:2157-2164.
[2] Giovanni Manente. High performance integrated solar combined cycles with minimum modifications to the combined cycle power plant design. Energy Conversion and Management, 111 (2016) 186–197.
[3] Giovanni manente. Optimum choice and placement of concentrating solar power technologies in integrated solar combined cycle systems. Renewable Energy, 96 (2016) 172-189.
[4] Mario Amelio. An evaluation of the performance of an integrated solar combined cycle plant provided with air-linear parabolic collectors. Energy, 69 (2014) 742-748.
[5] Lin Ruomou, Jin Hongguang. Integrated solar combined cycle power generation system. Gas Turbine Technology 2013;26(2):1-15.
[6] Allani Y.CO2 mitigation through the use of hybrid solar-combined cycles. Energy convers Manag., 1997;38:661–7.
[7] Kane M, Favrat D. Approche de conception et d'optimisation de centrale, solaire intégrée à cycle, combiné inspirée de la méthode du, pincement (partie 1: paliers de, récupération). (J). International Journal of Thermal Sciences, 1999, 59(1):9-16.

[8] Khaldi F. Energy and exergy analysis of the first hybrid solar-gas power plant in Algeria (C)// Ecos. 2012.
[9] Bakos GC,ParsaD.Technoeconomic assessment of an integrated solar combined cycle power plant in Greece using line-focus parabolic trough collectors. RenewEnergy 2013;60:598–603.
[10] Antoñanzas-TorresFernando, Sodupe-Ortega Enrique. Technical feasibility assessment of integrated solar combined cycle power plants in Ciudad Real (Spain) and Las Vegas (USA). In: Proceedings of the XVI congreso internacional de ingeniería de proyectos.Valencia;11–13deJulio de 2012.p.1282–891.
[11] Reddy V S, Kaushik S C, Tyagi S K. Exergetic analysis of solar concentrator aided coal fired super critical thermal power plant (SACSCTPT) (J). Clean Technologies and Environmental Policy, 2013, 15(1):133-145.
[12] Cau Giorgio, Cocco Daniele, Tola Vittorio. Performance and cost assessment of integrated solar combined cycle systems(ISCCSs) using CO2 as heat transfer fluid. Solar Energy,2012;86:2975–85.
[13] Feldhoff JanFabian. Direct steam generation(DSG) – technology overview. SFERA summer school, Almerá(Spain);28June2012.
[14] Mohamed AHEl-sayed. Solar supported steam production for power generation in Egypt. Energy Policy,2005;33:1251–9.
[15] Livshits Maya, Kribus Abraham. Solar hybrid steam injection gas turbine (STIG) cycle. Sol Energy 2012;86:190–9.
[16] Yuanyuan Li, Yongping Yang. Thermodynamic analysis of a novel integrated solar combined cycle (J). Applied Energy, 2014, 122:133-142.
[17] Nezammahalleh H, Farhadi F, Tanhaemami M. Conceptual design and techno-economic assessment of integrated solar combined cycle system with DSG technology (J). Solar Energy, 2010, 84(9):1696-1705.
[18] B. Kelly, U. Herrmann, M.J. Hale, Optimization studies for integrated solar combined cycle systems, in: Proceedings of Solar Forum 2001, Solar Energy: The Power to Choose, 2001. Apr 21e25; Washington DC, USA.